
O.V. BOKOTEY, V.V. VAKULCHAK, A.A. BOKOTEY, I.I. NEBOLA

Faculty of Physics, Uzhhorod National University
(46, Pidgirna Str., Uzhhorod 88000, Ukraine; e-mail: bokotey_ov@ukr.net)

MANIFESTATION OF POINT DEFECTS IN THE ELECTRONIC STRUCTURE OF $\text{Hg}_3\text{Te}_2\text{Cl}_2$ CRYSTALS

UDC 539

*Within the score of the density functional theory, we investigate the impact of point defects on the electronic structure of $\text{Hg}_3\text{Te}_2\text{Cl}_2$ crystals, by using the supercell model $[2 \times 2 \times 1]$. The *ab initio* calculations for defect-free and defective $\text{Hg}_3\text{Te}_2\text{Cl}_2$ crystals in the LDA approximation are performed for the first time, by using the quantum-chemical software package SIESTA. The studied crystal possesses an indirect band gap. According to the analysis of the obtained data, the indirect gap is equal to 2.628 eV, while the direct gap is 2.714 eV. The influence of vacancy defects on the conductive and optical properties of $\text{Hg}_3\text{Te}_2\text{Cl}_2$ crystals is discussed in detail. The tellurium and chlorine vacancy defect states indicate the presence of additional energy levels below the bottom of the conduction band edge. We have shown that only tellurium vacancies produce the additional energy levels in a vicinity of the valence band maximum. It is found that the presence of point defects in $\text{Hg}_3\text{Te}_2\text{Cl}_2$ changes the direction of optical transitions. Therefore, the defective crystal is a direct gap semiconductor. The satisfactory agreement with the experimental data is obtained.*

Keywords: band structure, point defects, gap, absorption edge, optical transitions.

1. Introduction

$\text{Hg}_3\text{X}_2\text{Y}_2$ (X = S, Se, Te; Y = F, Cl, Br, I) compounds are crystallized into the corderoite structure. The acentricity of a crystal structure of the mentioned crystals is one of the reasons to forecast their possible application also as a non-linear optical material. The structure and its relation to the fundamental physical properties of these compounds is a very interesting subject for theoretical studies due to the expected possibilities of their practical usage. It is worth to mention that the main structural feature of $\text{Hg}_3\text{X}_2\text{Y}_2$ mercury chalcogenhalogenides is the tendency to the formation of various polymorphic modifications due to the great conformational capacity of the mercury-chalcogen component [1–4]. Additionally, in this class of materials, the point defects of a lattice struc-

ture are the significant contributors to their applications.

The optical properties of $\text{Hg}_3\text{X}_2\text{Y}_2$ crystals such as the refractive index, optical activity, electrooptical effect, visible and IR transparencies, photoconductivity, optical nonlinearity *etc.*, make them promising nanomaterials for nonlinear applications [1–7]. They are of great interest for practical applications in electronic and acoustic-optical devices: modulators, elements for dynamic holography, recording, information storage, deflectors, and other devices based on the phenomenon of the interaction of light beams.

The main key to the better understanding of a material lies in the physics of defects. Apart from influencing the electronic properties, the point defects mediate the self- and the dopant-diffusion. Thus, the investigation of point defects is of a great physico-technological interest. It should be noted that the

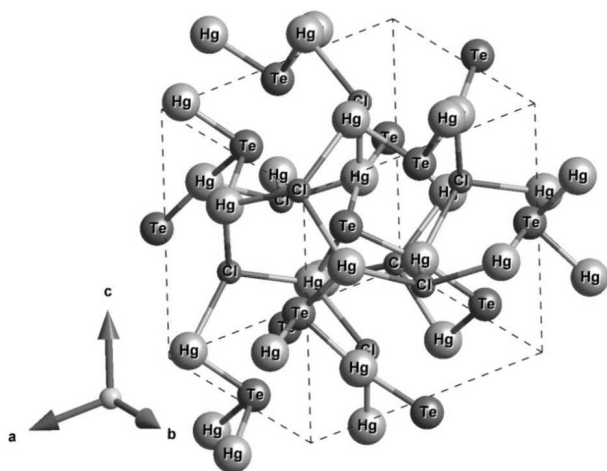


Fig. 1. Crystal structure of $\text{Hg}_3\text{Te}_2\text{Cl}_2$

DFT calculation is an effective approach to the determination of crystal properties, as it involves assumptions about the electronic structure and atomic interactions and creates new opportunities for the design of new materials with promising properties. Physical properties of semiconductors depend strongly on minor changes in a crystal structure caused by defects or imperfections.

The present paper is aimed at the studies of the band structure of $\text{Hg}_3\text{Te}_2\text{Cl}_2$ crystals, by using the DFT approach. It focuses on two aspects: one is the comparing of the electronic structures for defective and defect-free $\text{Hg}_3\text{Te}_2\text{Cl}_2$, the other is the role of vacancy defects in the band gap formation. In the first part, the structural and electronic properties of $\text{Hg}_3\text{Te}_2\text{Cl}_2$ crystals are discussed. Next, the origin of Te and Cl vacancy defects and their influence on the electronic structure are studied. Such studies have not been carried out earlier for $\text{Hg}_3\text{Te}_2\text{Cl}_2$ crystals.

2. Calculations

The *ab initio* calculations of the energy band structure are performed within the density functional theory (DFT) formalism [8–9], by using the SIESTA software package on the basis sets of linear combinations of the atomic orbitals. The exchange-correlation interaction was considered in the local density approximation (LDA) [10–11]. We have used the Hubbard correction to obtain a better band gap value that is mostly underestimated by LDA. The procedure of calculations uses first-principles atomic norm-

conserving pseudopotentials [12–14] of atomic electronic configurations: Hg – [Xe] $4f^{14}5d^{10}6s^2$, Te – [Kr] $4d^{10}5s^25p^4$, Cl – [Ne] $3s^23p^5$. The specified states belong to the valence shells, [Kr], [Ne] – to the core. The integration over the irreducible part of the Brillouin zone was conducted, by using the method of special k -points. The Brillouin zone was sampled with special k -points of a $2 \times 2 \times 1$ grid for structure calculations. The total and partial densities of electron states were determined by the modified tetrahedral method, for which the energy spectrum and wave functions were calculated on a k -grid. The calculation is based on the $\text{Hg}_3\text{Te}_2\text{Cl}_2$ structure, in which the space group is $T^5 - I2_13$. The cell parameter is $a = b = c = 9.33 \text{ \AA}$ and $\alpha = \beta = \gamma = 90^\circ$. Finally, we carried out the geometric optimization, which minimized the total energy of the system simultaneously with the forces acting on atoms. The theoretical values of crystallographic parameters are in good agreement with available experimental data.

3. Crystal Structure

$\text{Hg}_3\text{X}_2\text{Y}_2$ compounds are crystallized in a structure of the $\alpha\text{-Hg}_3\text{S}_2\text{Cl}_2$ type. It is realized in the cases where the chalcogen anion size is more than the halogen anion size: S^{2-} (0.182 nm), Se^{2-} (0.193 nm), Te^{2-} (0.211 nm) $>$ Cl^- (0.181 nm); Te^{2-} (0.211 nm) $>$ Br^- (0.196 nm). The main feature of this structural type is the existence of $(\text{Hg}_3\text{X}_2)_{2n}^{2+}$ infinite chains from $[\text{XHg}_3]$ trigonal pyramids connected by the mercury atoms which are common for two pyramids. These chains are united in a three-dimensional framework. In its octahedral cavities, the halogen ions are localized [4]. One specific case for such kind of crystals is the existence of isomorphic substitutions in the chalcogen and halogen anion sublattices. A special feature of all studied modifications of $\text{Hg}_3\text{X}_2\text{Y}_2$ compounds is the stronger ordering of the anions as compared to the cations, owing to the strong covalent $\text{Hg} = \text{X}$ bonds. These bonds form various configurations with almost the same fixed bond lengths.

$\text{Hg}_3\text{X}_2\text{Cl}_2$ (X = Se, Te) gyrotropic crystals are characterized by a structure with spiral chains. The atoms are located on the upward or downward double spiral in the structure (Fig. 1). A characteristic feature of all compounds is the presence of two sets of octahedral spirals with different radii and twist-

ing directions. They are located side by side, oriented in the same direction, and consistently alternated. The spiral, which is twisted counterclockwise, has a larger radius. The steps of both spirals are identical. There are some groups of atoms in the structure of $\text{Hg}_3\text{X}_2\text{Y}_2$ crystals, which act as an optically active chromophore. $[\text{HgX}_2\text{Cl}_4]$ octahedra form spiral chains with a triple spiral axis in the (111) direction of the elementary cube. There are three spirals of each type along the (111) direction, and they are at some distance from one another in $\text{Hg}_3\text{Te}_2\text{Cl}_2$ [1]. The interaction of spirals with opposite direction is increased, and the change of a rotation sign is due to this fact. The sign of $\text{Hg}_3\text{Te}_2\text{Cl}_2$ crystal rotation is caused by the strong influence of X^{VI} and Y^{VII} atoms on the symmetry of the local crystal field and the polarization medium as a result.

The structure of $\text{Hg}_3\text{Te}_2\text{Cl}_2$ crystals is characterized by the following set of possible nuclear positions: $\text{C}_2(4)$, $\text{C}_2(6)$, and $\text{C}_1(12)$ [3]. Atoms occupy the positions: 12Hg (b) $[x \ 0 \ 0.25]$ ($x = 0.31$), 8Te (a) $[x \ x \ x]$ ($x = 0.28$), 8Cl (a) $[x \ x \ x]$ ($x = 0.025$), which defines by the following set:

12B (2) – $\{x, 0, 1/4\}$, $\{1/2 - x, 0, 3/4\}$, $\{1/4, x, 0\}$, $\{0, 1/4, x\}$, $\{3/4, 1/2 - x, 0\}$, $\{0, 3/4, 1/2 - x\}$;
 8A (3) – $\{x, x, x\}$, $\{1/2 + x, 1/2 - x, -x\}$, $\{1/2 - x, -x, 1/2 + x\}$, $\{-x, 1/2 + x, 1/2 - x\}$.

It should be noted that the Hg^{2+} ion owns the considerable polarizing (deforming) action due to the completely populated shell of 18 electrons ($4s^2 4p^6 4d^{10} 4f^{14} 5s^2 5p^6 5d^{10}$). It is necessary to consider also the additional effect of a polarization: the anion, which is easily deformed, can create, maybe, the deforming action on a strongly deformed cation. This leads to the anion polarization growth. The additional effect of the polarization is characteristic of the ions having a 18-electron shell and increases on the subgroup from top to down: the deformation of electron shells increases with the radius of an ion [4]. There are two types of chemical bonds in the crystals under study: the covalent bonds between atoms of mercury and halides, and ionic bonds between atoms of mercury and halogens.

4. Results and Discussion

Real crystals always have certain defects or imperfections. Therefore, the arrangement of atoms in the volume of a crystal is far from being perfectly regu-

lar. The defects often introduce additional electronic states in the band gap and are also responsible for the mass transport. Their acceptor or donor levels control the Fermi level position, providing the p -type and n -type conditions necessary for electronic devices.

The simplest point defect is a vacancy, and such defects may arise either from the imperfect packing during the original crystallization or from thermal vibrations of the atoms at higher temperatures. In the latter case where the thermal energy due to vibrations is increased, there is always an increased probability that individual atoms will jump out of their positions with the lowest energy. The presence of point defects is important in the kinetics of diffusion and oxidation. It is known that the dominant lattice defect responsible for the ionic conductivity in $\text{Hg}_3\text{X}_2\text{Y}_2$ crystals is the anion vacancy. The anionic defect is a donor one, which increases the concentration of electrons. The presence of crystalline defects is undesirable, but certain types of defects are essential in the semiconductor manufacturing.

The calculated electronic structures of defect-free and defective $\text{Hg}_3\text{Te}_2\text{Cl}_2$ crystals are presented in Figs. 2–4. The band structure of $\text{Hg}_3\text{Te}_2\text{Cl}_2$ crystals is calculated along the direction that contains the highest number of high-symmetry points of the Brillouin zone (BZ): $\Gamma \rightarrow \text{P} \rightarrow \text{N} \rightarrow \text{H} \rightarrow \text{P} \rightarrow \text{X}' \rightarrow \Gamma \rightarrow \text{N}$. The coordinates of the special points of the BZ are (in units of the reciprocal lattice vectors): $\Gamma(0, 0, 0)$; $\text{P}(1/4, 1/4, 1/4)$; $\text{N}(0, 0, 1/2)$; $\text{H}(1/2, -1/2, 1/2)$; $\text{X}'(1/2, 1/2, -1/2)$. The Fermi level is taken to be 0.0 eV.

According to our results, the defect-free $\text{Hg}_3\text{Te}_2\text{Cl}_2$ crystal is an indirect-gap semiconductor with the calculated band gap width $E_{gi} = 2.628$ eV ($\text{N} \rightarrow \Gamma$), and the direct gap width is $E_{gd} = 2.714$ eV ($\Gamma \rightarrow \Gamma$). It is in good agreement to the experimentally obtained data [15]. Figure 5 shows the value of experimental absorption coefficient $\alpha(h\nu)$ near the energy gap for the $\text{Hg}_3\text{Te}_2\text{Cl}_2$ crystal and indicates the presence of both direct and indirect optical transitions in the studied crystals. The vacancies create an additional absorption peak near 2.5 eV in the experimentally obtained spectrum. The absorption coefficient increases sharply above 2.632 eV. The indirect gap has the value $E_g = 2.63$ eV, and the direct gap width is $E_{gd} = 2.82$ eV and correlate with theoretical data with the Hubbard correction.

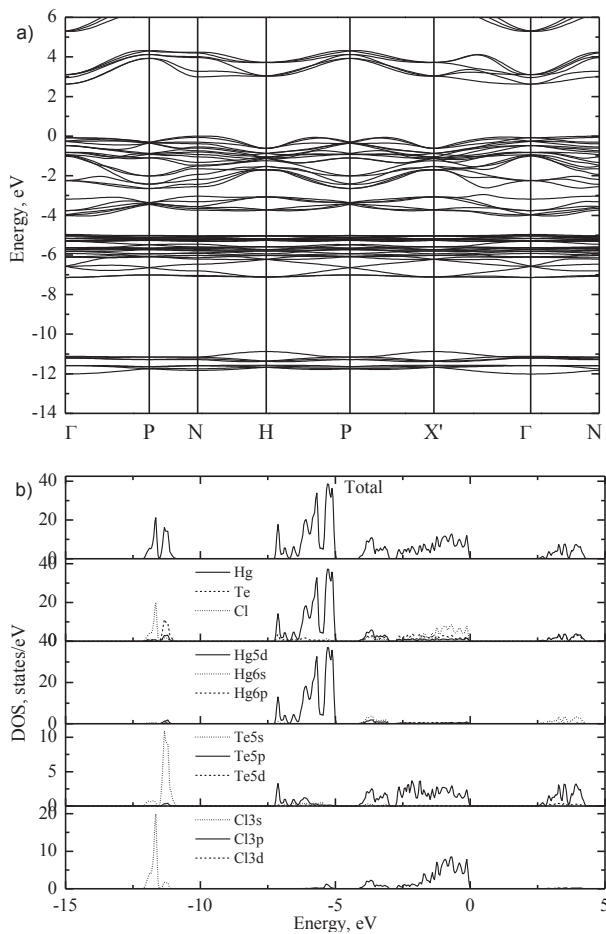


Fig. 2. Calculated electronic band structure (a), total and partial densities of states (b) for $\text{Hg}_3\text{Te}_2\text{Cl}_2$ crystals with the use of LDA + U

Figure 2, b shows DOS/PDOS for defect-free $\text{Hg}_3\text{Te}_2\text{Cl}_2$ calculated by the DFT. The conduction band is formed by the hybridization of Te p -states and Hg s -states. The top of valence band originates mainly from Te and Cl p -states with small contributions from the Hg s - and d -states. The energy window from -7 to -5 eV consists of the maximum contribution of Hg d -states with contribution of Te p -states.

In general, the whole region of valence states has a complex hybrid character caused by the interaction of all atoms species inherent to the investigated crystals.

The inclusion of the spin-orbit coupling leads to the removal of the degeneracy, splitting, and doubling of energy levels in Γ , X' , H, and P points of the Brillouin zone. Our analysis shows that the spin-orbit interac-

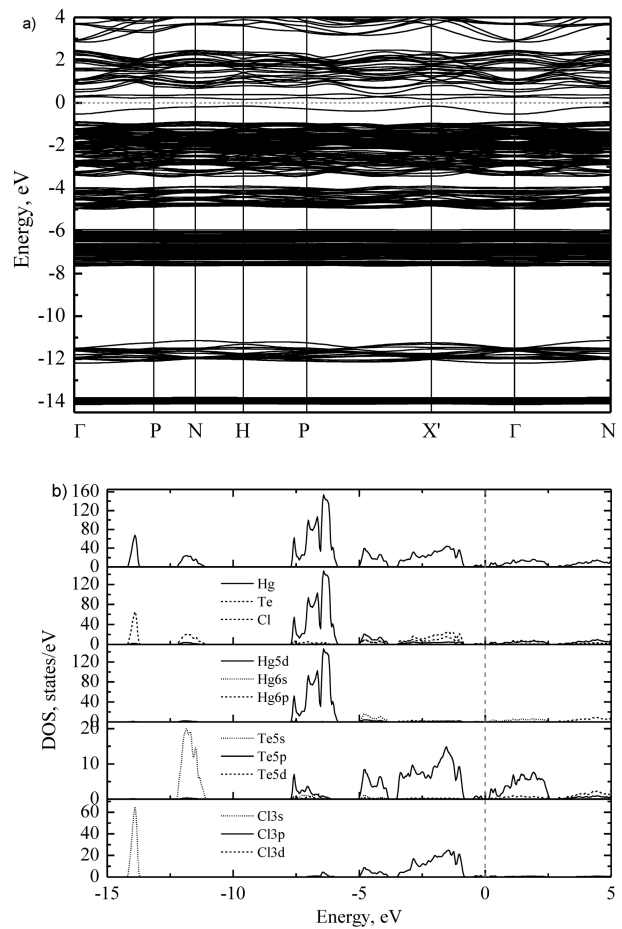


Fig. 3. Electronic structure (a), total and partial densities of states (b) for $\text{Hg}_3\text{Te}_2\text{Cl}_2$ crystals with Te vacancies in the supercell model $2 \times 2 \times 1$

tion slightly modifies the band gap value, direction of interband transitions, and energy position of some subbands of the valence band.

In addition, the interpretation of a crystal gyrotropy is obtained from the band structure calculations for $\text{Hg}_3\text{Te}_2\text{Cl}_2$ crystals [1]. They indicate the presence of direct and indirect interband transitions with regard for the exciton effects in the fundamental absorption edge. The analysis of the experimental observation of the optical activity in $\text{Hg}_3\text{Te}_2\text{Cl}_2$ crystals and DFT calculations [6, 16–18] shows that the magnitude and the dispersion of the rotatory ability are connected with direct interband transitions. The theoretical aspects of a gyrotropy are interpreted from expressions for the dielectric permittivity tensor and

the gyration tensor. This leads to the conclusion that the linear components play the main role and are connected with interband transitions. They define the $\rho(\lambda)$ spectral dependence near the fundamental absorption edge. Displacements (λ) with a change in the temperature reflects the temperature dependence of the band gap width in the studied crystals. So, the gyrotropy of $\text{Hg}_3\text{Te}_2\text{Cl}_2$ crystals has molecular nature and is associated with the induced asymmetrization of $[\text{HgTe}_2\text{Cl}_4]$ chromophores, which is determined by the space symmetry group of the crystals. Exciton effects give a significant contribution to the gyrotropy in the range of the fundamental absorption edge.

$[\text{HgTe}_2\text{Cl}_4]$ octahedra are the most deformed part of the structure, and the deformation degree of this structural complex caused by internal crystal field will determine the strength of transition rotation and the optical activity value of crystals. The value of specific rotation increases with the deformation. The transition of atoms $[\text{HgTe}_2\text{Cl}_4]$ octahedra in any of the excited electronic states makes contribution to the gyrotropy caused by the C_1 local symmetry group [1].

The rotation dispersion gives information about the band structure and dispersion laws of the valence and conduction bands. The analysis of the optical rotation curves for $\text{Hg}_3\text{Te}_2\text{Cl}_2$ crystals [1, 6] shows that they are smooth and exhibit no anomalies in the investigated range. It should be noted that the sharp growth of curves is observed, when approaching the absorption edge. This indicates that the rotation of $\text{Hg}_3\text{Te}_2\text{Cl}_2$ crystals is connected with direct interband transitions. But the participation of other electronic transitions, which are localized in the depth of the fundamental absorption, in the gyrotropy of $\text{Hg}_3\text{Te}_2\text{Cl}_2$ crystals is not excluded.

The absolute maxima of the valence band can be realized at the N point, and the absolute minimum of the conductive band is localized at the Γ point (transition $N \rightarrow \Gamma$). But the presence of vacancy defects changes the direction of interband transitions. The valence band maximum and the bottom of the conductive band are located at the center of the Brillouin zone. One can conclude that $\text{Hg}_3\text{Te}_2\text{Cl}_2$ crystals with Te and Cl vacancy defects are direct semiconductors (transition $\Gamma \rightarrow \Gamma$).

The shape of energy curves creating the valence band possesses the dispersion prevailingly at the P and Γ points, which reflects the contribution of the long-range potential formed predominantly by the

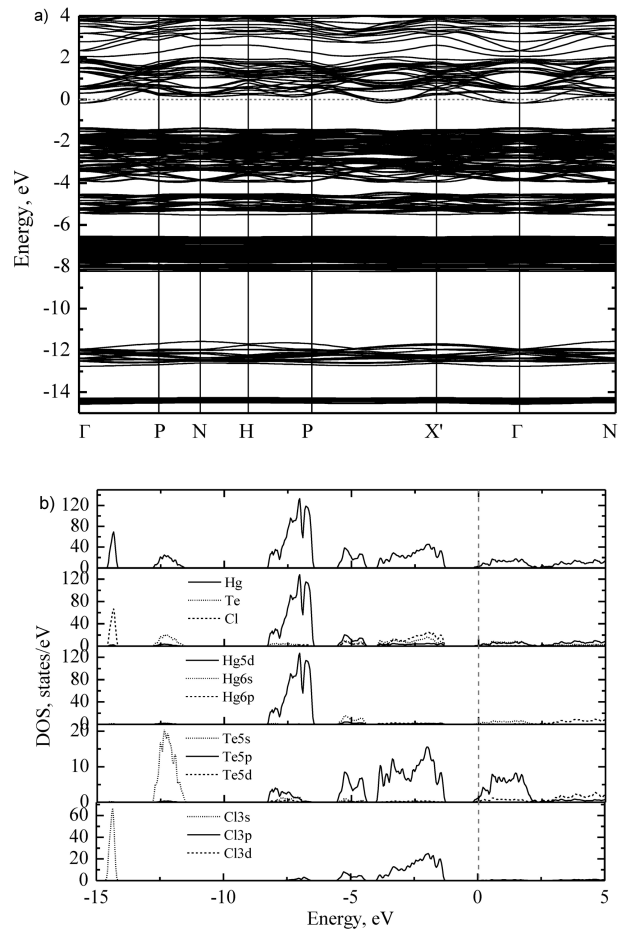


Fig. 4. Electronic structure (a), total and partial densities of states (b) for $\text{Hg}_3\text{Te}_2\text{Cl}_2$ crystals with Cl vacancies in the supercell model $2 \times 2 \times 1$

p -originated states of the both anions. Other high-symmetry points and directions of the Brillouin zone are less sensitive to the delocalization. The significant dispersion of the conductive band bottom is observed in the $X' - \Gamma \rightarrow N$ direction.

Comparing the defect-free and defective band structures shows that the Te and Cl vacancy defects give additional energy levels in the band gap. The Te vacancies give additional energy levels near the bottom of the conductive band and the top of the valence band. The top of the valence band is formed from Cl p -states and Te p -states. The bottom of the conductive band is originated by the hybridization of Te p - and d -states and Hg s -states (Fig. 3). Additional levels are created due to the hybridization of these

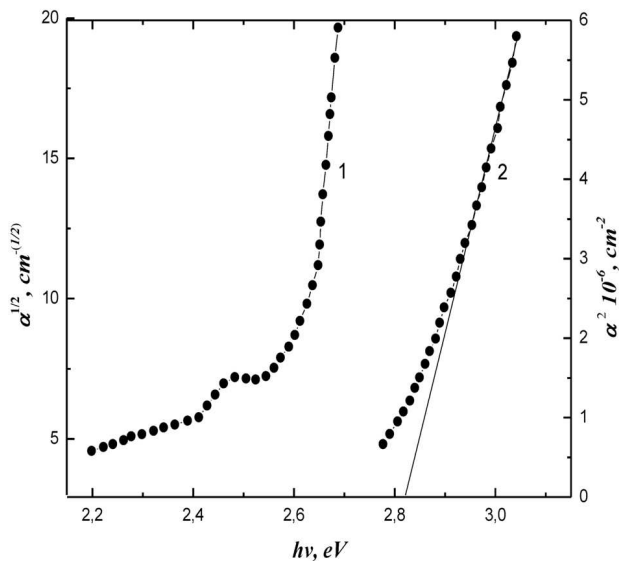


Fig. 5. Experimental spectral dependence of the absorption coefficient near the energy gap edge for $\text{Hg}_3\text{Te}_2\text{Cl}_2$

orbitals. The Cl vacancies create additional levels only lower the conductive band (Fig. 4). There are no changes near the valence band maximum, and the behavior of the defective crystals is similar to the defect-free $\text{Hg}_3\text{Te}_2\text{Cl}_2$ crystals in this case.

Vacancies are classified as a fundamental native point defect and introduce deep levels inside the band gap. Figures 3 and 4 show that the point defects of Te and Cl vacancies introduce defect levels inside the $\text{Hg}_3\text{Te}_2\text{Cl}_2$ fundamental band gap. The extended band states of anion vacancies are donors, and the conduction band edge states have the p -character, while the valence band edge states have the hybridized p - and s -character.

It should be noted that the vacancy defects shift the conductive band to the lower energy, by decreasing the energy gap. The additional energy levels appear, by creating an additional trap for charge carriers. The tellurium and chlorine atoms have anion character, but the neutral vacancies are formed to keep the system not charged. Vacancy defects create new defects-associated energy states intra the band gap or introduce resonant states in the areas of the valence bands or conductive bands. The anion vacancy is a donor, so the Fermi energy level is moved into the conduction band. Thus, there is a significant filling of the defect state. The important electronic transition is induced at the visible range with peaks, which were produced

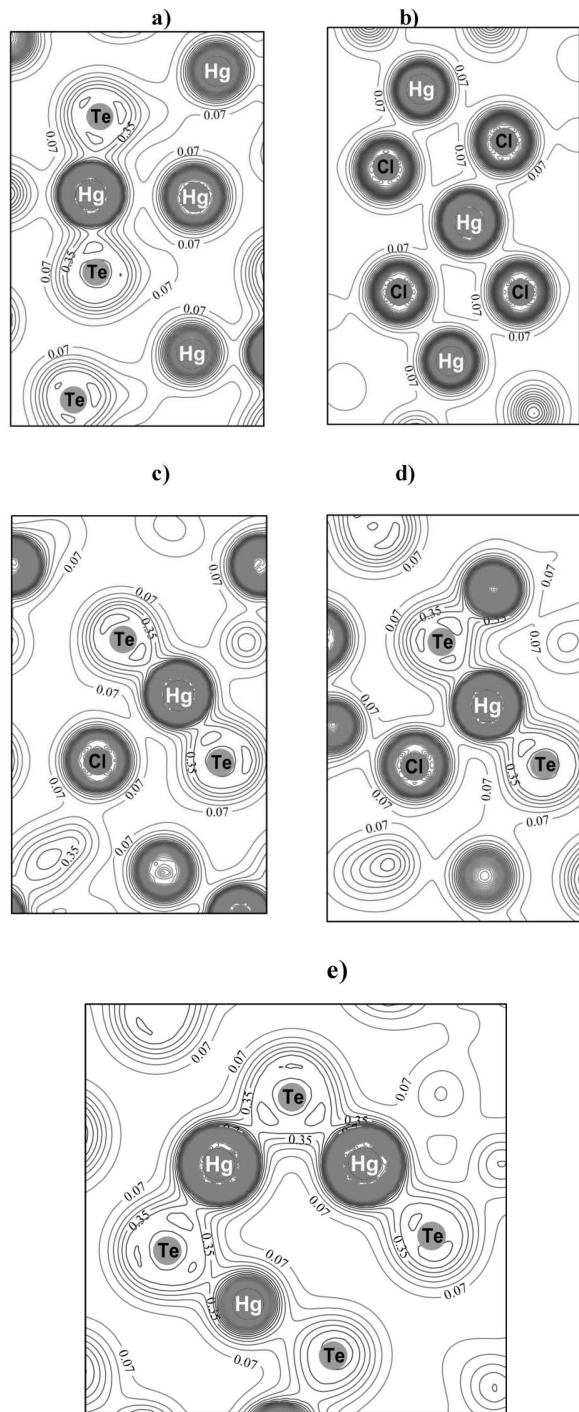


Fig. 6. Spatial distribution maps of the charge density in $[\text{HgTe}_2\text{Cl}_4]$ octahedra: along the Hg-Te bond line (a); through Hg and Cl atoms (b); through non-bridging Cl atoms and Hg, Te atoms (c); through bridging Cl atoms and Hg, Te atoms (d); along the Hg-Te-Hg-Te spiral chains (e)

by anions point defects. The decrease of the electron transition energy from the valence band to the conduction band may be responsible for the visible light optical absorption in $\text{Hg}_3\text{Te}_2\text{Cl}_2$ crystals. The dispersion of the energy bands versus the direction of the Brillouin zone for a defected structure possesses the same feature, as observed for the perfect crystal.

Analyzing the calculated energy spectra for defective $\text{Hg}_3\text{Te}_2\text{Cl}_2$ crystals, one can see that the lowered energy level is localized at the $X' - \Gamma$ direction and formed by Te p -states. This is the additional energy level creating the bottom of conduction band. The top of valence band is formed from the hybridized s -states of cations and p -states of anions. The p -states of tellurium atoms are dominating in both bands and affect the band structure near the Fermi level.

The calculated energy spectra demonstrate changes in the band gap and in the positions of all energy levels of the valence and conductive bands. Such changes of the electron energy spectra obviously testify to an important role of the electron-phonon interaction in the nature of the spontaneous polarization of $\text{Hg}_3\text{Te}_2\text{Cl}_2$ crystals.

The origin of the chemical bonding can be elucidated from the calculated partial density of states (PDOS). The charge density maps (Fig. 6) describe the distribution of electrons in $\text{Hg}_3\text{Te}_2\text{Cl}_2$ crystals and allow us to compare the distribution nature in different crystallographic planes. Figure 6 shows the presence of covalent bonds in $\text{Hg}_3\text{Te}_2\text{Cl}_2$ caused by the hybridization of chalcogen and halogen p -states and mercury s -states. In addition, they demonstrate the electronic density distribution in the studied crystals in the plane intersecting along $\text{Hg}=\text{Te}$ and $\text{Hg}=\text{Cl}$ bonds. Localized maxima of the electronic density on cation-anion bonds are connected among themselves by the common contours of constant charge density and characterize the covalent component of chemical bonds. Ionic binding is characterized by the increase in charge around anions and the decrease in charge at the covalent bond between ions.

5. Conclusions

In this paper, the first-principles calculations are performed to study the effects of Te- and Cl-vacancies on the electronic properties of $\text{Hg}_3\text{Te}_2\text{Cl}_2$ crystals. The vacancy defects create the optical states localized in the band gap. In the case of Te vacancies, the addi-

tional energy levels near the both valence band and conduction band are observed, but Cl vacancies create only additional energy levels lower the conductive band. It is established that all additional levels are formed due to the hybridization of cations and anions. The existence of vacancy defects changes the direction of the interband transitions. The anion vacancies modify the energy band structure, which affects the electronic and optical properties of $\text{Hg}_3\text{Te}_2\text{Cl}_2$ crystals. In addition, the anion vacancies influence greatly the geometry structure of surrounding atoms, and the great relaxation of the surface occurs, which results in the alteration of electronic properties for $\text{Hg}_3\text{Te}_2\text{Cl}_2$ crystals. The electron density maps demonstrate the covalent $\text{Hg}=\text{Te}$ and ionic $\text{Hg}=\text{Cl}$ bond characters. Our results also indicate that the theoretical study can provide an important information and a good prediction of semiconductor properties. Therefore, the study of the influence of vacancy defects on the electronic structure of $\text{Hg}_3\text{Te}_2\text{Cl}_2$ is helpful for the more profound understanding of the origin of crystal defects in the corderoite-type structures.

1. O.V. Bokotey, Investigation of gyrotropic properties for $\text{Hg}_3\text{X}_2\text{Cl}_2$ ($X=\text{Se}, \text{Te}$) crystals, *J. Alloys Compd.* **678**, 444 (2016) [DOI: 10.1016/j.jallcom.2016.04.018].
2. O.V. Bokotey, Theoretical calculations of refractive properties for $\text{Hg}_3\text{Te}_2\text{Cl}_2$ crystals, *Nanoscale Res. Lett.* **11**, 251 (2016) [DOI: 10.1186/s11671-016-1476-8].
3. O.V. Bokotey, K.E. Glukhov, I.I. Nebola, and A.A. Bokotey, First-principles calculations of phonons and Raman spectra in the $\text{Hg}_3\text{Te}_2\text{Cl}_2$ crystals, *J. Alloys Compd.* **669**, 161 (2016) [DOI: 10.1016/j.jallcom.2016.02.005].
4. O.V. Bokotey, I.P. Studenyak, I.I. Nebola, and Yu.V. Minets, Theoretical study of structural features and optical properties of the $\text{Hg}_3\text{S}_2\text{Cl}_2$ polymorphs, *J. Alloys Compd.* **660**, 193 (2016) [DOI: 10.1016/j.jallcom.2015.11.086].
5. R. Nitsche, Crystal growth and optical properties of mercury-telluro-chloride, $\text{Hg}_3\text{Te}_2\text{Cl}_2$, *Mater. Res. Bull.* **7**, 679 (1972) [DOI: http://10.1016/0025-5408(72)90056-6].
6. Yu.V. Voroshilov, Z.P. Hadmashi, and V.O. Hudolii, Production and natural optical activity of mercury chalcogenhalogenides, *Neorg. Mater.* **17**, 2022 (1981).
7. O.V. Bokotey, Refractive index behavior of mercury chalcogenhalogenides $\text{Hg}_3\text{X}_2\text{Hal}_2$, in *Proceedings of Ukrainian-German Symposium on Physics and Chemistry of Nanostructures and on Nanobiotechnology, Kyiv, Ukraine, September 21–25, 2015*, p. 140.
8. P. Hohenberg and W. Kohn, Inhomogeneous electron gas, *Phys. Rev. B* **136**, 864 (1964) [DOI: 10.1103/PhysRev.136.B864].

9. W. Kohn and L.J. Sham, Self-consistent equations including exchange and correlation effects, *Phys. Rev.* **140**, A1133 (1965) [DOI: 10.1103/PhysRev.140.A1133].
10. D.M. Ceperley and B.J. Alder, Ground state of the electron gas by a stochastic method, *Phys. Rev. Lett.* **45**, 566 (1980) [DOI: 10.1103/PhysRevLett.45.566].
11. J.P. Perdew and A. Zunger, Self-interaction correction to density-functional approximations for many-electron systems, *Phys. Rev. B.* **23**, 5048 (1981) [DOI: 10.1103/PhysRevB.23.5048].
12. J.M. Soler, E. Artacho, J.D. Gale, A. García, J. Junquera, P. Ordejón, and D. Sánchez-Portal, The SIESTA method for ab initio order- N materials simulation, *J. Phys.: Condens. Matter.* **14**, 11, 2745 (2002), arXiv: cond-mat/0111138v1 [cond-mat.mtrl-sci].
13. G.B. Bachelet, D.R. Hamann, and M. Schlüter, Pseudopotentials that work: From H to Pu, *Phys. Rev. B* **26**, 8, 4199 (1982).
14. C. Hartwigsen, S. Goedecker, and J. Hutter, Relativistic separable dual-space Gaussian pseudopotentials from H to Rn, *Phys. Rev. B* **58**, 7, 3641 (1998) [DOI: 10.1103/PhysRevB.58.3641].
15. Z.P. Hadmashi and L.M. Suslikov, Absorption edge of $\text{Hg}_3\text{Te}_2\text{Cl}_2$ crystals, *Fiz. Tverd. Tela* **26**, 2, 592 (1984).
16. O.V. Bokotey, V.V. Vakulchak, and I.I. Nebola, Electronic structure of mercury chalcogenhalogenides $\text{Hg}_3\text{X}_2\text{Hal}_2$, in *Proceedings of Ukrainian-German Symposium on Physics and Chemistry of Nanostructures and on Nanobiotechnology, Kyiv, Ukraine, September 21–25, 2015*, p. 139.
17. O.V. Bokotey, V.V. Vakulchak, and I.I. Nebola, Influence of defects on the band structure of $\text{Hg}_3\text{X}_2\text{Y}_2$ ($X = \text{S}, \text{Se}, \text{Te}$; $Y = \text{F}, \text{Cl}, \text{Br}, \text{I}$) crystals, in *Proceedings of the XXth International Seminar on Physics and Chemistry of Solids, Lviv, Ukraine, September 12–15, 2015*, p. 69.
18. O.V. Bokotey, V.V. Vakulchak, I.I. Nebola, and A.A. Bokotey, Band structure and optical transitions in the $\text{Hg}_3\text{Se}_2\text{Cl}_2$ crystals, *J. Phys. Chem. Sol.* **99**, 153 (2016) [DOI: 10.1016/j.jpcs.2016.08.016].

Received 05.04.16

O.V. Бокотей, В.В. Вакулчак,
О.О. Бокотей, І.І. Небола

ПРОЯВ ТОЧКОВИХ
ДЕФЕКТІВ В ЕЛЕКТРОННІЙ
СТРУКТУРІ КРИСТАЛІВ $\text{Hg}_3\text{Te}_2\text{Cl}_2$

Резюме

Представлено результати розрахунків в рамках теорії функціонала густини для дослідження впливу точкових дефектів на електронну структуру кристалів $\text{Hg}_3\text{Te}_2\text{Cl}_2$ з використанням моделі суперкомірки $[2 \times 2 \times 1]$. Вперше проведено *ab initio* розрахунки для бездефектних та дефектних кристалів $\text{Hg}_3\text{Te}_2\text{Cl}_2$ в наближенні локальної густини, використовуючи квантово-хімічний програмний пакет SIESTA. Досліджуваний кристал є непрямозонним напівпровідником. Згідно з аналізом отриманих даних, величини непрямого та прямого переходів становлять 2,628 eV та 2,714 eV відповідно. Вплив дефектів вакансій на провідні та оптичні властивості кристалів $\text{Hg}_3\text{Te}_2\text{Cl}_2$ обговорюється в деталях. Дефектні стани вакансій телуру та хлору створюють додаткові енергетичні рівні нижче дна зони провідності. Результати дослідження показують, що тільки вакансії телуру створюють додаткові енергетичні рівні в околі вершини валентної зони. Встановлено, що присутність точкових дефектів в кристалах $\text{Hg}_3\text{Te}_2\text{Cl}_2$ змінює напрямок оптичних переходів і тому дефектний кристал є прямозонним напівпровідником. Одержано задовільне узгодження з експериментальними даними.